Perspective: Single polymer mechanics across the force regimes

Omar A. Saleh

Citation: J. Chem. Phys. **142**, 194902 (2015); doi: 10.1063/1.4921348
View online: http://dx.doi.org/10.1063/1.4921348
View Table of Contents: http://aip.scitation.org/toc/jcp/142/19
Published by the American Institute of Physics

Perspective: Single polymer mechanics across the force regimes

Omar A. Saleh[a)]
Materials Department and BMSE Program, University of California, Santa Barbara, California 93106, USA

(Received 13 March 2015; accepted 8 May 2015; published online 18 May 2015; publisher error corrected 24 July 2015)

I review theoretical and experimental results on the force-extension response of single polymers, with a focus on scaling pictures of low-force elastic regimes, and recent measurements of synthetic and biological chains that explore those regimes. The mechanical response of single polymers is an old theoretical problem whose exploration was instigated by the curious thermomechanical behavior of rubber. Up until the 1990s, the main utility of those calculations was to explain bulk material mechanics. However, in that decade, it became possible to directly test the calculations through high-precision single-chain stretching experiments (i.e., force spectroscopy). I present five major single-chain elasticity models, including scaling results based on blob-chain models, along with analytic results based on linear response theory, and those based on freely jointed chain or worm-like chain structure. Each model is discussed in terms of the regime of force for which it holds, along with the status of its rigorous assessment with experiment. Finally, I show how the experiments can provide new insight into polymer structure itself, with particular emphasis on polyelectrolytes. © *2015 AIP Publishing LLC.* [http://dx.doi.org/10.1063/1.4921348]

I. INTRODUCTION

The elastic, or force-extension, response of a single polymer holds direct technological importance because it determines the mechanical properties of polymeric materials: single-chain elasticity is famously invoked to explain the mechanics of elastomeric polymer networks (rubbers).[1,2] It is also used to understand the structure of polymer brushes,[3,4] as well as to model the dynamics of chain relaxation.[5] Polymer elasticity also holds relevance to mechanobiology; for example, the response of cytoskeletal structures to external stress can be linked to the elastic response of individual filaments of, e.g., actin.[6] Further, recently developed methods exploit the elastic response of single chains to sense the stresses generated by cells.[7,8]

Quantification of chain behavior in these situations requires knowledge of the shape of the single-chain elastic response function. There has been a long and rich history of theoretical consideration of this problem—indeed, for over half a century, the only direct consideration of the problem was theoretical. Because of the dominance of entropy in defining polymer elasticity, prediction of the single-chain elastic response is well-suited to methods of statistical mechanics. As a consequence, even introductory statistical mechanics textbooks, which otherwise do not mention polymers, commonly include "entropic spring" problems.[9]

Direct experimental data on single-polymer elasticity were, for a long time, absent. Instead, the elastic response function was indirectly estimated by combining measurements of the mechanics of rubber with models that separated the contributions of single-chains from that of the network as a whole.[10–15] This changed with the invention in the 1990s of ingenious experimental techniques that permitted direct measurement of single-chain mechanics (i.e., "force spectroscopy" techniques).[16–18] In their initial application, these techniques utilized relatively large forces, and thus probed only the tail end of the elastic response function. It is only in the past few years that lower-force regimes have begun to be investigated.[19–22] Along with permitting direct measurement of chain mechanics, the introduction of single-chain stretching techniques also prompted a philosophical change: force-extension models, initially conceived as components of a broader theory of material mechanics, began to be used in conjunction with high-resolution experimental data to give new information on microscopic details of polymer structure.

In this perspective, I begin in Sec. II by reviewing key theoretical models describing single-chain mechanics, including some notes on the history of the problem. In Sec. III, I briefly discuss the experimental methodologies that permit measurements of single-chain elasticity, with special attention given to low-force measurements. Finally, in Sec. IV, I review recent progress in exploring the low-force regime, including discussions both of new methods that leverage fluctuations to estimate elasticity and of the use of elasticity to determine the structure of charged chains.

II. MODELS OF FORCE-EXTENSION BEHAVIOR

A. Historical impetus: Rubber elasticity

The single-chain elasticity problem has its roots in experimental observations that are over 200 yr old (further historical details can be found in Refs. 1 and 2). In 1805, John Gough discovered that natural rubber gives off heat when stretched, and that stretched rubber contracts when heated.[23] These thermomechanical observations were confirmed and expanded in work by Joule and Kelvin in the 1850s.[24,25] A microscopic explanation for the effect was not clarified

a)Electronic mail: saleh@engineering.ucsb.edu

until Staudinger's classic 1920 paper, which put forth the hypothesis that rubber (among other materials) was made up of a network of long chains.[26] The key physical insight, that the entropic origin of rubber thermoelasticity could be found in the configurational freedom of the many bonds of the constituent macromolecules, was made by Meyer *et al.* in 1932.[27] Thus was born the entropic spring concept: polymer chains resist stretching because the number of available configurations of the chain decreases with increasing extension. This conceptual advance was also prescriptive. It indicated that models of elasticity could be built, given estimates of the number of configurations of the chain in various states.

B. The entropic spring

Quantification of the entropic spring occurred immediately after the work of Meyer *et al.*:[27] Guth and Mark in 1934, and Kuhn in 1936, calculated the number of states available to a random-walk chain to find the first single-chain force-extension prediction.[10,11] I briefly derive this result using the fluctuation-dissipation relation,[28] as I will make use of this approach again later. Define the ensemble average polymer end-to-end extension in the direction of applied force to be $\langle X \rangle$, which takes on non-zero values in response to a constant applied force $\vec{f} = f\hat{x}$. For small values of f, the response will be linear, $\langle X \rangle = \alpha f$, with α being the mechanical susceptibility. Fluctuation-dissipation then dictates $\langle X^2 \rangle = k_B T \alpha$, where $k_B T$ is the thermal energy, giving

$$\langle X \rangle = \frac{\langle X^2 \rangle}{k_B T} f. \tag{1}$$

In the classic entropic spring, the mean-squared polymer extension in the direction of applied force is found using the random walk result: $\langle X^2 \rangle = \langle R^2 \rangle /3 = N\ell^2/3$, where R is the rms end-to-end extension in three dimensions, and in which the polymer is modeled as a phantom (self-crossing) chain of N inextensible links, each of length ℓ and connected by free joints. This gives

$$\langle X \rangle = \frac{N\ell^2}{3k_B T} f. \tag{2}$$

This equation was successful both in its qualitatively correct accounting of rubber's thermoelastic effects and in quantitatively predicting rubber elasticity at low applied stress.

C. The freely jointed chain (FJC)

The classic entropic spring model suffers from an obvious defect: it indicates an infinitely extensible chain, whereas the extension of a real chain must asymptote to the contour length (that is, we cannot have $\langle X \rangle > N\ell \equiv L$). This issue was rectified by many of the same authors who first derived Eq. (2): Kuhn and James and Guth made the connection between the orientation of a stiff link under applied tension to Langevin's solution for the ensemble average orientation of a spin in a magnetic field.[13,14] This gave an elastic model, valid for all forces, for a phantom FJC,

$$\langle X \rangle = L\left[\coth\left(\frac{f\ell}{k_B T}\right) - \frac{k_B T}{f\ell}\right]. \tag{3}$$

The limiting behavior of Eq. (3) is of interest. The form of Eq. (3) immediately implies a characteristic force scale, $f_c \equiv k_B T/\ell$, that is dictated by the length of the link, ℓ. Then, two regimes can be discerned: at low forces, $f \ll f_c$, the entropic spring result Eq. (2) is recovered. At high forces, $f \gg f_c$, the asymptotic approach of extension to contour length is linear in inverse force,

$$\langle X\,(f \gg k_B T/\ell)\rangle \approx L\left(1 - \frac{k_B T}{f\ell}\right). \tag{4}$$

Early success was claimed for Eq. (3) in its ability to account for rubber elasticity at higher stresses.

D. The worm-like chain (WLC)

With the rubber elasticity problem mainly solved, further consideration of single-polymer mechanics was delayed (with one exception, discussed in Sec. II E) until the 1990s. The situation changed due to experimental innovations, which stringently tested the FJC model (Eq. (3)), and found that it failed. In 1992, Smith *et al.* showed that the elastic response of long double-stranded DNA molecules showed clear deviations from the FJC prediction.[16] The experiments were performed in the high force limit, $f > k_B T/\ell$, and thus really rejected only the asymptotic regime, Eq. (4). Thus, the experiment indicated a failure in the FJC model of the polymer (i.e., the idea of having rigid links joined by free joints), but not of the entropic spring prediction (Eq. (2)), which is independent of the microscopic structural assumption.

Stimulated by these experiments, Marko and Siggia reconsidered the single-chain elastic problem, modeling the polymer as a WLC, or persistent chain, with exponential backbone correlations.[29] That is, given unit tangent vector $\hat{t}(s)$ at contour position s, the correlation function is taken to be $\langle \hat{t}(s+x) \cdot \hat{t}(s) \rangle = \exp(-|x|/l_p)$, where l_p is the persistence length (note that a WLC can be mapped onto a statistically equivalent FJC by choosing $\ell = 2l_p$). The key difference is that the WLC model captures the ability of the chain to deform on short length scales, i.e., to undergo bending fluctuations with wavelength less than $2l_p$, which are unphysically cut off in the FJC model. By determining the energy of exciting the chain's deformation modes under tension and applying equipartition, Marko and Siggia calculated the force-extension relation in the high-force ($f \gg k_B T/l_p$) limit, finding

$$\langle X\,(f \gg k_B T/l_p)\rangle \approx L\left(1 - \sqrt{\frac{k_B T}{4 f l_p}}\right). \tag{5}$$

This model predicts an asymptotic approach to contour length proportional to the square-root of inverse force (compare with the linear proportionality of the FJC, Eq. (4)).

The Marko-Siggia elastic model matches high-force stretching data on a variety of polymers in which electrostatic interactions are either missing or negligible; this includes double-stranded DNA,[30] polypeptides,[18] synthetic chains,[21] and, at certain large salt concentrations, single-stranded nucleic acids.[19,22] Indeed, I am unaware of a single-polymer

experiment which has convincingly shown FJC elastic behavior. This makes intuitive sense: the exponential correlation function, and not the FJC's step-like correlation function, is nearly universally a good descriptor of neutral polymer structure, because of a chain's intrinsic rigidity (as in double-stranded DNA) or because of the cumulative sequential effect of backbone bond rotations (as occurs in flexible chains).[31]

While the Marko-Siggia elastic model captures a great deal of experimental reality, deviations from Eq. (5) are expected: for example, recent work convincingly argues that chains will undergo a transition from WLC to FJC elastic behavior at a relatively large force,[32,33] though this has not been observed experimentally. More generally, Eq. (5) will fail because it assumes inextensible chains, whereas real chains always show at least some extensibility, which can be included, to first-order, through straightforward extensions of Eq. (5).[34]

Extending Eq. (5) to lower forces has also been accomplished, though not in an exact fashion. Assuming the polymers act as phantom chains, one expects Eq. (2) to hold in the low-force limit. Marko and Siggia provided an approximate expression that interpolates between the high and low force regimes (Eqs. (5) and (2), respectively),[29] while others provide more exact expressions.[35] That said, only recently have experiments truly probed the low-force behavior, as discussed in Sec. III.

E. The scaling approach and blob models

Between the times of introduction of Eqs. (3) and (5), Flory and others elucidated the nature of swollen chains whose self-crossings were not negligible,[1] notably finding that $\langle R^2 \rangle \sim N^{2\nu}\ell^2$, with $\nu \approx 3/5$. In 1976, de Gennes pointed out that Eq. (1) still applies to swollen chains,[36] giving a new force/extension prediction,

$$\langle X \rangle \approx \frac{N^{6/5}\ell^2}{3k_BT} f. \tag{6}$$

This result immediately pointed out the existence of a novel elastic regime. Pincus noted that Eq. (6) is not extensive in chain length, while the high-force extension must regain an extensive dependence on N, indicating the existence of an intermediate force regime in which the extension is extensive with N, but that retains sensitivity to swelling.[37] He introduced the tensile screening length, $\xi \equiv k_BT/f$, and formulated a scaling argument in which the chain extension was taken to depend on the product of R and a power-law function Φ of the dimensionless ratio R/ξ, setting $\langle X \rangle = R\Phi(R/\xi)$. This approach differs from the prior elastic models, which are derived directly from methods of statistical thermodynamics, but which require assumptions of phantom chain or linear response behavior. The Pincus model is commonly viewed as corresponding to a polymer acting as a chain of blobs of size ξ, with each blob acting as a swollen random walk on length scales shorter than ξ, but with the blob chain pulled straight in the direction of force.[37] By enforcing an extensive force-extension relation, the scaling model predicts

$$\langle X \rangle \sim f^{1/\nu - 1} \tag{7}$$

which gives a 2/3 power law dependence for $\nu \approx 3/5$, while retaining the expected linear dependence on force for a phantom chain with $\nu = 1/2$.

F. Summary of the theoretical picture: Force and length scales of elasticity

At this point, I have presented the major single-chain elasticity predictions, Eqs. (2)-(7); it remains to synthesize them. Following Netz,[38] I present a qualitative and intuitive overview of the transitions between the various regimes, which is summarized in Fig. 1. These considerations are fully compatible with recent simulation results on single-chain elastic regimes.[39,40]

The tensile screening length, $\xi = k_BT/f$, provides a useful way to build up a scaling picture of the elasticity regimes. A change in elastic behavior will occur whenever the tensile screening length passes through a structural length scale of the polymer. Two such length scales have been introduced: the chain's random walk extent, R, and the length scale of local stiffness, ℓ. In fact, only one of these is needed for ideal (phantom) chains, as there is no transition at $\xi = R$. Instead, an ideal chain is expected to follow canonical

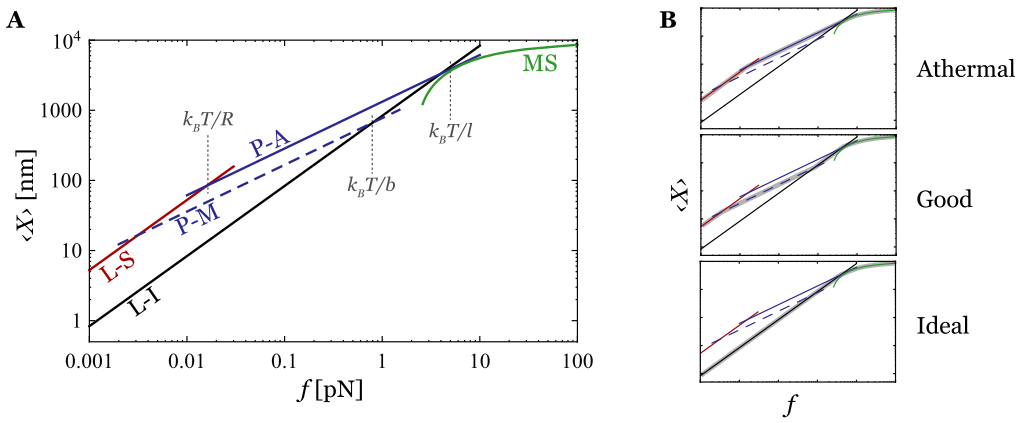

FIG. 1. Regimes of elasticity of a single neutral chain. (a) Force-extension predictions for a polymer of contour length 10^4 nm and Kuhn length $\ell = 1$ nm, with various choices for the extent of swelling. L-I: linear response of an ideal chain (Eq. (2)), L-S: linear response of a swollen chain (Eq. (6)), P-A (P-M): Pincus regime in athermal (good) solvent (Eq. (7)), and MS: Marko-Siggia model (Eq. (5)). (b) Expected elastic trajectories for chains in various solvents, shown as thick gray lines highlighting the relevant elastic laws from (a).

entropic spring behavior, Eq. (2), both in the linear response regime ($\xi > R$) and the intermediate regime ($R > \xi > \ell$). The transition to asymptotic behavior occurs at $\xi = \ell$, beyond which the Marko-Siggia WLC model (Eq. (5)) should describe the elasticity.

For real (swollen) chains, another length scale must be introduced, corresponding to the length beyond which self-avoidance becomes statistically significant—that is, for moderate intra-chain repulsions, a short polymer will behave ideally ($\nu = 1/2$), while a long chain will be swollen ($\nu = 3/5$).[31,41] The chain extent at which this conversion happens is termed the thermal blob size, b, and can be related to the monomer excluded volume factor. Note that in the limit of strong intra-chain repulsions, swelling will commence immediately, with $b \approx \ell$; this is termed the athermal solvent regime, which can be differentiated from the good solvent regime for which $b > \ell$.[31]

Swollen-chain elasticity thus exhibits three potential transitions points (at $\xi = R$, b, and ℓ), see Fig. 1. At the lowest forces, linear response dictates the elastic behavior will follow Eq. (6). As force increases to the intermediate regime, $R > \xi > b$, a swollen chain will obey the Pincus elastic model, Eq. (7), with $\nu = 3/5$. In good solvents ($b > \ell$), the swollen chain will undergo another transition at $\xi = b$, from Pincus behavior back to canonical entropic spring elasticity; athermal chains with $b = \ell$ will not show this effect. Finally, beyond the point $\xi = \ell$, the chain is nearly perfectly straight, with looping nearly entirely disallowed. Here, one expects an asymptotic approach to contour length, likely following the Marko-Siggia model, Eq. (5).

III. FORCE-EXTENSION MEASUREMENTS

Experimental developments have had a clear and decisive effect in prompting an understanding of single-polymer elasticity—indeed, the experiments of Gough and Joule instigated the first look into the subject. Here, I will briefly describe single-molecule mechanical measurements. I will not discuss details of exactly how such experiments are setup and calibrated (a variety of reviews discuss this; see, e.g., Ref. 42). Instead, the goal is to determine the ability, or lack thereof, of single-molecule experiments to access the various elastic regimes discussed in Sec. II F.

Direct measurement of single-chain elasticity requires enormous sensitivity to both chain extension and applied tension. In length, the required sensitivity scales with the chain contour length—as can be seen in the equations presented above, the expected change in mean extension with force will increase for longer chains. This is why early experiments focused on chains with extremely long (16 μm or more) contour lengths.[16,17] That said, even for such chains, lengths must be measured with better than 100 nm accuracy, while for shorter chains, accuracies approaching 1 nm are required. The required scale of force can be estimated from the magnitude of the aforementioned transition at $\xi = \ell$, corresponding to $f = k_B T/\ell \approx 4$ pN, assuming a flexible chain with Kuhn length $\ell \approx 1$ nm.

The three major single-molecule stretching approaches (the optical trap, the atomic force microscope (AFM), and the magnetic tweezer[42]) share common experimental design features. All three methods utilize a micron-scale probe (e.g., a dielectric colloid, a magnetic colloid, or a micromachined cantilever) fixed at one end of the polymer, with the other end attached to an immobile surface. The probe transduces an external field (a focused laser light field, a magnetic field, or bending stresses) into a stretching force while its position is tracked optically. Force calibration typically proceeds by leveraging the high-resolution measurement of position: in particular, by tracking the perturbations of probe position caused by thermal fluctuations (or external flow), the relation between applied force and location can be determined, frequently by modeling the system as a harmonic oscillator and using the perturbations to quantify the effective spring constant.

While similar in design, the various measurement approaches have differing abilities to access the elastic regimes. The main limitation is in applying very small forces: in each of their typical implementations, the lower bound of stable force is 10 pN for the AFM, 1 pN for the optical trap, and 0.1 pN for the magnetic tweezer. Thus, the AFM cannot access any but the highest-force stretching regime, and none of the elastic transitions. A typical optical trap does better, but still does not get a full decade below the 4 pN threshold, thus limiting the ability to discern power-law behavior. Thus, only the magnetic stretching technique can reliably access a large portion of the intermediate force regime, $R > \xi > \ell$. Accordingly, as will be detailed below, only that technique has achieved experimental observation of various polymer elastic regimes.[19,21]

IV. EXPLORATIONS OF INTERMEDIATE ELASTICITY

The magnetic stretching technique was introduced in 1996, with early use focused on studies of supercoiled DNA and DNA/protein interactions.[17,43–45] The realization of the application to (relatively) low-force behavior occurred later, with the first direct observation of intermediate-regime ($R > \xi > \ell$) elasticity reported in 2009 in experiments on single-stranded DNA (ssDNA).[19] Several works prior to 2009 investigated the elasticity of single-stranded nucleic acids (ssNAs),[46–48] including with magnetic tweezers.[49] However, the focus of those works was either on intra-strand basepairing, on high-force elasticity, or on salt regimes too low to remove the obscuring effects of electrostatic stiffening.

Since the 2009 observation, intermediate elasticity has been explored in a variety of systems, shown to be powerful in the application to polyelectrolytes, and revealed some subtleties unanticipated by the simple scaling theories.

A. ssNAs and polyelectrolyte behavior

Double-stranded DNA (dsDNA) has played a key role in advancing polymer research; notably, it was used in the experimental studies that motivated and confirmed the Marko-Siggia WLC elasticity model (Eq. (5)).[16,30] DNA's experimental utility arises from a combination of features: its high charge insures extremely good aqueous solubility, while modern biotechnological capabilities permit facile synthesis of very long chains with both high monodispersity

and a variety of specifically placed chemical modifications. However, dsDNA's extremely large Kuhn length ($\ell \approx 100$ nm) places the transition to intermediate elasticity at a very low force ($k_BT/\ell \approx 0.04$ pN). Thus, ssNAs are the prototypical system for exploring intermediate elasticity—they share many of the same experimentally useful features, yet have a Kuhn length, in high salt, of only ≈1 nm, placing the transition to intermediate elasticity at an accessible 4 pN. An experimental complication of working with ssNAs is the possibility of strong attractive interactions between monomers mediated by basepairing interactions; however, a variety of techniques have been developed to either remove basepairing in mixed-sequence ssNAs through reactions with molecules that bind the bases[19,49] or to synthesize ssNAs of homogeneous sequence that lack complementary bases.[22,48,50]

Thus, for many of the same reasons dsDNA was used in the first experiments demonstrating WLC force/extension behavior, ssDNA was used in the first experiments demonstrating Pincus behavior:[19] single-molecule stretching data on ssDNA in relatively high salt conditions (1 M NaCl) show a pronounced low-force power-law elasticity regime extending over more than a decade in force, and with an exponent of roughly 0.6-0.65 (Fig. 2). That the exponent was near to, but below, the scaling value of 2/3 was anticipated in theoretical considerations which showed that observing $\gamma = 2/3$ would only occur for extraordinarily long chains.[51]

Both ssDNA and ssRNA elasticities are extremely salt-dependent,[19,22,48,49,52] as would be expected given the high intrinsic flexibility and high charge of those chains. At salt concentrations near 3 M, the swollen regime disappears, and ideal elastic behavior is observed, indicative of a theta point of the system (Fig. 2). As the salt concentration decreases below 1 M, the intermediate elastic regime persists but shifts to progressively lower forces.[19,22] This is indicative of electrostatic repulsion increasing the effective stiffness of the chain—indeed, from the scaling prediction discussed above, the transition out of the intermediate elastic regime should occur around k_BT/ℓ, thus the shift to lower forces can be used to quantify the increase in ℓ. This analysis indicates that $\ell \sim 1/\sqrt{c} \sim r_D$, where c is the concentration of monovalent salt and r_D is the solution Debye length.[19,22] This result agrees with only one of the two prevailing models for polyelectrolyte structure: it disagrees with the Odijk-Skolnick-Fixman (OSF) prediction ($\ell \sim r_D^2$)[53,54] but agrees with a supposition of de Gennes *et al.*,[55] later quantified by Barrat and Joanny,[56] that predicts a linear dependence on Debye length, $\ell \sim r_D$. The linear dependence stands in contrast to single-molecule stretching results on dsDNA,[57] which agree with the quadratic OSF result. In fact, a crossover in behavior between intrinsically stiff polymers (such as dsDNA) and flexible ones (such as ssDNA) is predicted by the Barrat-Joanny calculation,[56] which could rectify the results.

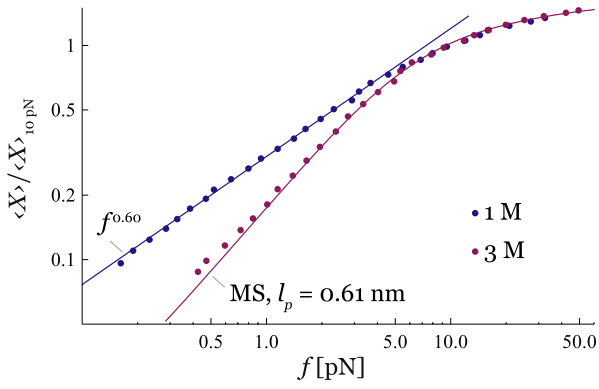

FIG. 2. Elastic response of chemically denatured mixed-sequence ssDNA at [NaCl] = 1 M (blue) and 3 M (purple).[19] Both curves are normalized by the extension at 10 pN to remove contour length variations that obscure comparison. The 1 M data show swollen chain (Pincus) behavior, with best-fit exponent noted. The 3 M data are near to a solution theta point and are fit to a numerical version of the Marko-Siggia model, due to Bouchiat *et al.*,[35] that interpolates between the expected high-force (Eq. (5)) and low-force (Eq. (2)) behavior. The best-fit persistence length is noted. Adapted with permission from Saleh *et al.*, Phys. Rev. Lett. **102**, 068301 (2009). Copyright 2009 The American Physical Society.

The role played by the solution Debye length in controlling ssNA elasticity agrees with a recent picture of flexible chain structure termed the "snake-like chain," or SLC.[58] This picture, formally equivalent to the Barrat-Joanny model,[58] was motivated by a variety of simulation results that indicated flexible chains are not well-described by a single persistence length over all scales, but rather by a dual-regime picture in which the chain has some short-length-scale flexibility that is relatively unaffected by electrostatics, followed by a long-length-scale structure that is stiffened by electrostatic repulsion.[59–63] The crossover between these scales appears, in simulations, to vary linearly with Debye length,[63] in agreement with the single-chain elasticity experiments on ssNAs.[19,22] Further confirmation of this picture arises from the anomalous elasticity of ssNAs in the high force ($f > k_BT/\ell$) regime, which do not follow the WLC prediction, Eq. (5), consistent with flexible polyelectrolytes not having a canonical persistence length.[19,22,48,49] Indeed, this connection has been strengthened in two ways: First, recent simulations of polyelectrolyte elasticity both reproduce the anomalous force-extension behavior and display non-exponential tangent-vector correlations.[64,65] Second, an analytical model by Toan and Thirumalai that assumes power-law, rather than exponential, tangent vector correlations is able to predict the shape of the ssNA force-extension behavior at high forces.[63] That said, power-law correlations have neither been directly confirmed experimentally nor explained from a microscopic viewpoint, and so are likely best viewed as provisional.

B. Thermal blobs and the onset of swelling

ssNA elasticity shows only two of the scaling regimes—the Pincus blob and high-force behaviors[19,22]–and thus behaves over a wide range of salt as a polymer in athermal solvent (Fig. 1). This indicates that, for ssDNA, the thermal blob size coincides with the Kuhn length ($b \approx \ell$). This coincidence of scales is expected for a polymer whose statistical monomers have spherically symmetric interactions—which is indeed the expected case for a chain dominated by electrostatics.[21] In contrast, the thermal blob size should become larger than the Kuhn length for rod-like monomers,[21] where the interactions along the chain differ from those orthogonal to it. Many neutral chains in a good solvent should behave as if they have rod-

like monomers, since for such chains interactions along the backbone are dominated by bond rotational freedom, while excluded-volume interactions (in good solvent) are defined by sterics, two different physical mechanisms whose asymmetry leads to rod-like behavior.

This basic viewpoint was tested in single-molecule elasticity measurements of poly(ethylene glycol) (PEG),[21] a neutral polymer with a high degree of aqueous solubility that is commonly used in anti-fouling applications. Force-extension curves of long-chain PEG indeed showed a high-force Marko-Siggia behavior, an intermediate-force linear behavior, and, at the lowest accessible forces, a slight increase in extension beyond the extrapolation of the previous linear behavior (Fig. 3). This slight swelling is consistent with that expected for Pincus-like swollen behavior, and thus indicates the transition from swollen chain behavior to ideal behavior at $f \approx k_B T/b$.

The appearance of swollen behavior in PEG elastic curves in buffered water occurs only at the extreme low end of available forces, and only persists for a relatively short force regime.[21] On its own, this observation would not convincingly demonstrate swollen-chain behavior. However, careful modification of solution conditions turned up key supporting evidence: by tuning the solvent quality with added salt, a theta point was reached in which the small swollen regime disappeared, without modification of the ideal intermediate regime (Fig. 3). This strongly supports the contention that the onset of swelling was indeed observed, and thus that single-molecule force-extension curves of PEG display, in good solvent, all three accessible scaling regimes.

More recently, a second system was found to show similar onset-of-swelling behavior: homopolymer ssDNAs, particularly with sequence poly(dA), are known to have strong nearest-neighbor base-stacking interactions, causing poly(dA) to have rod-like statistical monomers. Thus, as with PEG,

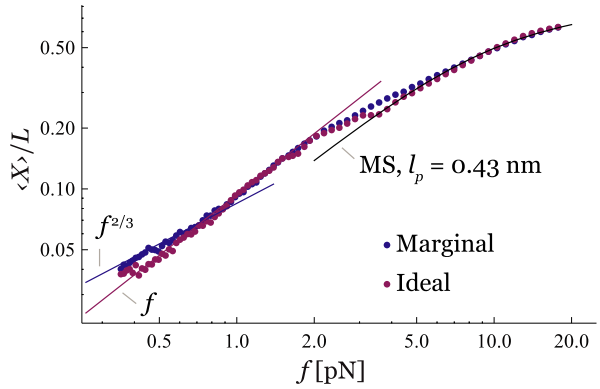

FIG. 3. Elastic response of poly(ethylene glycol), PEG, in good solvent (10 mM phosphate buffer) and ideal conditions (10 mM phosphate buffer with 1 M KCl).[21] Both curves are normalized by their apparent contour length to facilitate comparison. Both curves match over almost the entire range, except for a clear swelling at low force (<0.5 pN) in the good data. There is also a small deviation near 4 pN, apparently due to a variation in secondary structure formation in the chain.[21] MS: best fit of Eq. (5) to the high-force data. Power-laws are overlaid (not fit) to indicate swollen and ideal behavior. Adapted with permission from Dittmore *et al.*, Phys. Rev. Lett. **107**, 148301 (2011). Copyright 2011 The American Physical Society.

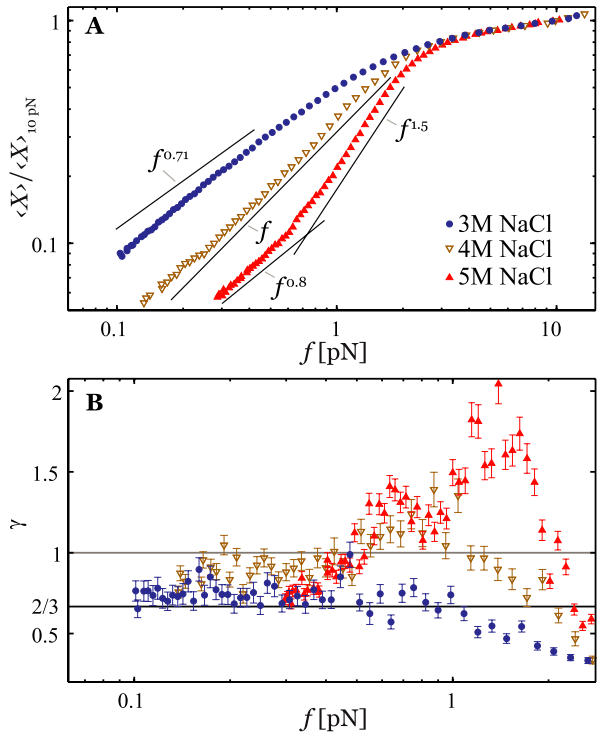

FIG. 4. (a) Elastic response of homogeneous-sequence, poly(dA), and ss-DNA in a variety of NaCl concentrations.[50] All curves are normalized by the extension at 10 pN to facilitate comparison. The data indicate a salt-driven transition from swollen-chain behavior at 3 M (similar to the 1 M data in Fig. 2) to a good-solvent behavior at 5 M (similar to the data in Fig. 3). Various power-laws are shown for comparison. (b) Estimate of effective local power-law exponent, γ, found from analyzing the fluctuations from the data shown in part (a) using Eq. (10). Adapted with permission from McIntosh *et al.*, Biophys. J. **106**, 659 (2014). Copyright 2014 Elsevier.

an observable thermal blob regime is expected, and indeed occurs: poly(dA) at molar monovalent salt concentrations displays two distinct elastic regimes (Fig. 4), roughly consistent with intermediate-force ideal behavior transitioning to a lower-force regime displaying swollen chain behavior.[50] poly(dA) elasticity deviates from the scaling expectation that the intermediate-ideal regime will show linear elasticity and the swollen regime will display a 2/3 power-law. However, the power-law exponents show the right qualitative trend, in that the ideal-like regime has a larger exponent than the lower-force swollen-like regime.

The single-molecule elasticity measurements of PEG and poly(dA)[21,50] (Figs. 3 and 4), two very different polymers that show a similar set of three elastic regimes, provide the best existing experimental evidence for the scaling view of elasticity discussed in Sec. II F.

C. Advances in exponent estimates

Confidently resolving power-law behavior over a limited range of the independent parameter (here, force) is a delicate experimental matter. For example, for limited-range power-law elasticity, it is difficult to extract exponents from direct fits to force-extension data, as it is not obvious *a priori* which points to actually include in the fitting procedure. Experimental identification of elastic regimes is thus aided

by exploiting all aspects of the measured data to check for self-consistency using alternate methodologies.

Recently, one such alternate methodology has been developed based on analysis of the fluctuations in polymer extension.[50] This approach avoids potential errors in hand-picking force regimes, as it allows the intrinsic thermal fluctuations of the chain end to report on the elastic behavior within the ensemble of thermally accessed polymer extensions. The method follows from the fluctuation-dissipation theorem: at equilibrium at a non-zero force f, a "local" susceptibility $\alpha(f)$ can be defined that captures the chain's linear response to small changes in force $f \to f + df$ and related to the variance in extension

$$\alpha(f) \equiv \left.\frac{d\langle X\rangle}{df}\right|_f = \frac{\langle X^2\rangle_f}{k_BT}. \tag{8}$$

Taking a power-law dependence of extension on force with exponent γ, the slope is $d\langle X\rangle/df = \gamma\langle X\rangle/f$, meaning the effective power-law exponent can be estimated from a single measurement of the mean and variance of the extension through

$$\gamma(f) = \frac{f\langle X^2\rangle_f}{k_BT\langle X\rangle_f}. \tag{9}$$

This can be further simplified. In the magnetic tweezer, the applied force can be calibrated by measuring both the extension and the *lateral* fluctuations of the probe particle, $\langle Y^2\rangle$, through the relation $f = k_BT\langle X\rangle/\langle Y^2\rangle$.[17] The effective, local power-law exponent is then found from a simple ratio of variances

$$\gamma(f) = \frac{\langle X^2\rangle_f}{\langle Y^2\rangle_f}. \tag{10}$$

A major benefit of Eq. (10) is that it does not rely on knowledge of the mean extension of the chain. Thus, the resulting exponent estimate is indeed independent of the estimate found from direct force-extension fitting, so the method is useful as a orthogonal consistency check. That said, there are a variety of constraints to this approach: First, it only holds true in the absence of significant noise from other sources, with the major concern being the rotational freedom of the probe particle itself, which typically becomes significant at forces of $\lesssim$0.1 pN. Second, it assumes the experiment measures probe position quickly enough to resolve the thermal variance, which can require correcting the measured variance for the finite bandwidth of the instrument.[66,67] Finally, the method (and particularly the fluctuation-dissipation relation) only works if the response is indeed linear over the range of the fluctuations. At very low forces, the fluctuations can grow so large as to access the non-linear response regime. It is likely a more nuanced theoretical approach can be developed that permits exponent estimates even in large-fluctuation regime, but this has not yet been seriously considered.

The fluctuation method, Eq. (10), has been applied to the stacked poly(dA) chains that show multi-power-law behavior;[50] see Fig. 4(b). As shown, the fluctuation-based estimates track the exponents found from fitting, and also do an excellent job at capturing subtle shifts in exponents as the polymer transitions between elastic regimes. The data shown also indicate the tendency for the stacked poly(dA) chains to have power-law elasticity exponents that deviate from the scaling predictions—whereas a transition in exponent from 2/3 to 1 is expected, the measured exponents are closer to 0.8 and 1.2–1.5. The reason for this deviation is unclear, but could be due to fluctuations in the polymer structure: the poly(dA) chain is expected to be a statistical co-polymer of stacked and unstacked segments, rather than a homogeneously structured chain.[50,68]

V. CONCLUSION AND OUTLOOK

The single-polymer elasticity problem has been advanced in three distinct time periods: the first, in the 1930s and 1940s, took place after Staudinger's macromolecular hypothesis[26] became accepted, leading to the introduction of the canonical entropic spring[10,11] (Eq. (2)) and FJC[13,14] (Eq. (3)) models. A second era includes only the period in the 1970s when de Gennes[36] and Pincus[37] put forth elastic models that accounted for swollen polymer behavior (Eqs. (6) and (7)). The third era was instigated by the introduction of experimental techniques to stretch single chains in the 1990s, leading to the first direct testing of force-extension predictions, the development of new models (notably the Marko-Siggia WLC model[29]; Eq. (5)), and the establishment of the broad scaling view of elasticity summarized in Sec. II F and Fig. 1.

The third era of single-molecule elasticity research is still ongoing, particularly as recent results continue to clarify the various regimes of elastic behavior and the models that apply in each regime. Notably, there is one elastic regime that has not been directly confirmed by single-molecule manipulation—the linear response regime (Eqs. (2) and (6) for ideal and real polymers, respectively). The existence of this regime is not in question. However, new information would be gained by direct observation of a low-force linear elastic regime, and particularly by the measurement of the crossover of a swollen chain from the linear response to Pincus elasticity. By the scaling logic described above, measurement of this crossover would result in an estimate of the chain's radius of gyration, R. One could thus imagine a single pulling experiment that would measure all regimes of elasticity, resulting in estimates of polymer structure on all scales, from local stiffness, ℓ, through to R, in a highly direct and efficient fashion. However, there are significant experimental hurdles to accessing the ultra-low force regime, which will occurs for forces $f \lesssim k_BT/\ell\sqrt{N}$ $\approx$ 0.04 pN, using the chain parameters from Fig. 1. Notably, the highly fluctuating polymer configuration will have large steric constraints due to interactions with the surfaces to which it is tethered, biasing the ensemble of available configurations. These could be reduced by using microscopic, needle-like tethering points that minimize steric interaction with the polymer. Recent work has begun to explore such tethering strategies,[69] so there does seem to be a feasible path forward.

Along with defining the scaling regimes of polymer elasticity, a second accomplishment of recent work is a reversal of focus: single-chain elasticity, long primarily viewed as a component of a *macroscopic* mechanical explanation of material behavior, can now be reliably exploited to give

microscopic information on polymer structure. The primary example of this is the body of work exploiting single-molecule elastic measurements to gain information on the structure of charged polymers. As discussed in Sec. IV A, single-molecule measurements provide direct evidence for the OSF-like behavior of the electrostatic effects on semi-flexible-chain stiffness (with dsDNA being the model system)[57] and for the non-OSF "snake-like" behavior of charged flexible chains (with ssNAs being the model system).[22,63,64] There are remaining open questions on polyelectrolyte structure that are good subjects for single-molecule investigation. These include the electrostatic behavior of chains whose non-electrostatic stiffness lies between that of single- and double-stranded DNA, and the behavior of weakly charged chains, about which theoretical work has already posited a range of structural regimes.[59,70] Finally, single-molecule methods are not limited to determining charged polymer structure; other complex structures, e.g., including branched or bottle brush configurations, are likely to be productive targets with these methods.

ACKNOWLEDGMENTS

I thank a range of excellent collaborators with whom this work was developed, including A. Dittmore, D. Jacobson, D. McIntosh, M. Stevens, and P. Pincus. I also thank M. Rubinstein, A. V. Dobrynin, and D. Thirumalai for helpful conversations. This work was supported by the NSF under Grant Nos. DMR-1309414, DMR-1006737, and PHY-0748564 and partially supported by the NSF's MRSEC program under Award No. DMR-1121053.

[1]P. J. Flory, *Principles of Polymer Chemistry* (Cornell University Press, 1953).
[2]L. R. G. Treloar, *The Physics of Rubber Elasticity* (Oxford University Press, 1975).
[3]P. de Gennes, Macromolecules **13**, 1069 (1980).
[4]S. Alexander, J. Phys. **38**, 983 (1977).
[5]P. G. de Gennes, *Scaling Concepts in Polymer Physics* (Cornell University Press, 1979).
[6]C. Storm, J. J. Pastore, F. C. MacKintosh, T. C. Lubensky, and P. A. Janmey, Nature **435**, 191 (2005).
[7]D. R. Stabley, C. Jurchenko, S. S. Marshall, and K. S. Salaita, Nat. Methods **9**, 64 (2012).
[8]M. Morimatsu, A. H. Mekhdjian, A. S. Adhikari, and A. R. Dunn, Nano Lett. **13**, 3985 (2013).
[9]C. Kittel and H. Kroemer, *Thermal Physics* (Macmillan, 1980).
[10]E. Guth and H. Mark, Monatsh. Chem. Verw. Teile Anderer Wiss. **65**, 93 (1934).
[11]W. Kuhn, Kolloid-Z. **76**, 258 (1936).
[12]E. Guth and H. M. James, Ind. Eng. Chem. **33**, 624 (1941).
[13]H. M. James and E. Guth, J. Chem. Phys. **11**, 455 (1943).
[14]W. Kuhn and F. Grün, Kolloid-Z. **101**, 248 (1942).
[15]W. Kuhn and F. Grün, J. Polym. Sci. **1**, 183 (1946).
[16]S. B. Smith, L. Finzi, and C. Bustamante, Science **258**, 1122 (1992).
[17]T. R. Strick, J.-F. Allemand, D. Bensimon, A. Bensimon, and V. Croquette, Science **271**, 1835 (1996).
[18]M. Rief, M. Gautel, F. Oesterhelt, J. M. Fernandez, and H. E. Gaub, Science **276**, 1109 (1997).
[19]O. A. Saleh, D. B. McIntosh, P. Pincus, and N. Ribeck, Phys. Rev. Lett. **102**, 068301 (2009).
[20]D. B. McIntosh, N. Ribeck, and O. A. Saleh, Phys. Rev. E **80**, 041803 (2009).
[21]A. Dittmore, D. B. McIntosh, S. Halliday, and O. A. Saleh, Phys. Rev. Lett. **107**, 148301 (2011).
[22]D. R. Jacobson, D. B. McIntosh, and O. A. Saleh, Biophys. J. **105**, 2569 (2013).
[23]J. Gough, Mem. Lit. Philos. Soc., Manchester **1**, 288 (1805).
[24]W. Thomson (Kelvin), Q. J. Pure Appl. Math. **1**, 57 (1857).
[25]J. P. Joule, Philos. Trans. **149**, 91 (1859).
[26]H. Staudinger, Ber. Dtsch. Chem. Ges. **53**, 1073 (1920).
[27]K. H. Meyer, G. v. Susich, and E. Valk, Kolloid-Z. **59**, 208 (1932).
[28]L. D. Landau and E. M. Lifshitz, *Statistical Physics*, Course of Theoretical Physics Vol. 5 (Elsevier, 1980).
[29]J. F. Marko and E. D. Siggia, Macromolecules **28**, 8759 (1995).
[30]C. Bustamante, J. F. Marko, E. D. Siggia, and S. Smith, Science **265**, 1599 (1994).
[31]M. Rubinstein and R. H. Colby, *Polymer Physics* (Oxford University Press, USA, 2003).
[32]L. Livadaru, R. R. Netz, and H. J. Kreuzer, Macromolecules **36**, 3732 (2003).
[33]A. V. Dobrynin, J. M. Y. Carrillo, and M. Rubinstein, Macromolecules **43**, 9181 (2010).
[34]T. Odijk, Macromolecules **28**, 7016 (1995).
[35]C. Bouchiat, M. D. Wang, J.-F. Allemand, T. Strick, S. M. Block, and V. Croquette, Biophys. J. **76**, 409 (1999).
[36]P. De Gennes, Macromolecules **9**, 587 (1976).
[37]P. Pincus, Macromolecules **9**, 386 (1976).
[38]R. R. Netz, Macromolecules **34**, 7522 (2001).
[39]H. P. Hsu and K. Binder, J. Chem. Phys. **136** (2012).
[40]L. Dai and P. S. Doyle, Macromolecules **46**, 6336 (2013).
[41]D. W. Schaefer, J. F. Joanny, and P. Pincus, Macromolecules **13**, 1280 (1980).
[42]K. C. Neuman and A. Nagy, Nat. Methods **5**, 491 (2008).
[43]J.-F. Allemand, D. Bensimon, R. Lavery, and V. Croquette, Proc. Natl. Acad. Sci. U. S. A. **95**, 14152 (1998).
[44]B. Maier, D. Bensimon, and V. Croquette, Proc. Natl. Acad. Sci. U. S. A. **97**, 12002 (2000).
[45]T. R. Strick, V. Croquette, and D. Bensimon, Nature **404**, 901 (2000).
[46]S. B. Smith, Y. J. Cui, and C. Bustamante, Science **271**, 795 (1996).
[47]M. Rief, H. Clausen-Schaumann, and H. E. Gaub, Nat. Struct. Biol. **6**, 346 (1999).
[48]Y. Seol, G. M. Skinner, and K. Visscher, Phys. Rev. Lett. **93**, 118102 (2004).
[49]M. N. Dessinges, B. Maier, Y. Zhang, M. Peliti, D. Bensimon, and V. Croquette, Phys. Rev. Lett. **89** (2002).
[50]D. B. McIntosh, G. Duggan, Q. Gouil, and O. A. Saleh, Biophys. J. **106**, 659 (2014).
[51]G. Morrison, C. Hyeon, N. M. Toan, B. Y. Ha, and D. Thirumalai, Macromolecules **40**, 7343 (2007).
[52]D. B. McIntosh and O. A. Saleh, Macromolecules **44**, 2328 (2011).
[53]T. Odijk, J. Polym. Sci., Polym. Phys. Ed. **15**, 477 (1977).
[54]J. Skolnick and M. Fixman, Macromolecules **10**, 944 (1977).
[55]P. G. de Gennes, P. Pincus, R. M. Velasco, and F. Brochard, J. Phys. **37**, 1461 (1976).
[56]J. L. Barrat and J. F. Joanny, Europhys. Lett. **24**, 333 (1993).
[57]C. G. Baumann, S. B. Smith, V. A. Bloomfield, and C. Bustamante, Proc. Natl. Acad. Sci. U. S. A. **94**, 6185 (1997).
[58]M. Ullner, J. Phys. Chem. B **107**, 8097 (2003).
[59]R. Everaers, A. Milchev, and V. Yamakov, Eur. Phys. J. E **8**, 3 (2002).
[60]T. T. Nguyen and B. I. Shklovskii, Phys. Rev. E **66**, 021801 (2002).
[61]M. Ullner and C. E. Woodward, Macromolecules **35**, 1437 (2002).
[62]J.-M. Y. Carrillo and A. V. Dobrynin, Macromolecules **44**, 5798 (2011).
[63]N. M. Toan and D. Thirumalai, J. Chem. Phys. **136**, 235103 (2012).
[64]M. J. Stevens, D. B. McIntosh, and O. A. Saleh, Macromolecules **45**, 5757 (2012).
[65]M. J. Stevens, D. B. McIntosh, and O. A. Saleh, Macromolecules **46**, 6369 (2013).
[66]W. P. Wong and K. Halvorsen, Opt. Express **14**, 12517 (2006).
[67]B. M. Lansdorp and O. A. Saleh, Rev. Sci. Instrum. **83**, 025115 (2012).
[68]Y. Seol, G. M. Skinner, K. Visscher, A. Buhot, and A. Halperin, Phys. Rev. Lett. **98** (2007).
[69]E. Pfitzner, C. Wachauf, F. Kilchherr, B. Pelz, W. M. Shih, M. Rief, and H. Dietz, Angew. Chem., Int. Ed. **125**, 7920 (2013).
[70]A. R. Khokhlov and K. A. Khachaturian, Polymer **23**, 1742 (1982).